6254 *Chem. Mater.* **2010,** *22,* 6254–6262
DOI:10.1021/cm101733h

CHEMISTRY OF MATERIALS
Article

A New Tetragonal Crystalline Polymorph of Lithium Octa-*n*-Butoxy-Naphthalocyanine (LiNc-BuO) Radical: Structural, Magnetic and Oxygen-Sensing Properties

Ramasamy P. Pandian,[†] Nandyala P. Raju,[‡] Judith C. Gallucci,[§] Patrick M. Woodward,[§] Arthur J. Epstein,[‡,§] and Periannan Kuppusamy*,[†]

[†]*Center for Biomedical EPR Spectroscopy and Imaging, Davis Heart and Lung Research Institute, Department of Internal Medicine,* [‡]*Department of Physics, and* [§]*Department of Chemistry, The Ohio State University, Columbus, Ohio 43210, United States*

Received June 21, 2010. Revised Manuscript Received September 21, 2010

The single-crystal structure, paramagnetic, and oxygen-sensing characteristics of a new tetragonal polymorph of lithium octa-*n*-butoxynaphthalocyanine, LiNc-BuO (T_g), is reported. The compound was synthesized as fine, diamond-shaped, neutral radical crystals by reacting octa-*n*-butoxynaphthalocyanine (Nc-BuO) with lithium metal in *n*-butanol. Single-crystal X-ray diffraction analysis revealed a saddle-shaped conformation of the molecule with a crystallographic 2-fold rotation axis in a tetragonal unit cell. This represents the first single-crystal, structurally characterized, lithium naphthalocyanine complex. Unlike the triclinic polymorph of LiNc-BuO (Pandian, et al. *J. Mater. Chem.* **2006**, *16*, 3609), the tetragonal (T_g) form of LiNc-BuO did not show the presence of large open channels in the crystalline packing. The magnetic susceptibility and EPR spectroscopic properties were in agreement with the X-ray crystal structure showing the existence of a high degree of spin exchange in the crystalline system. The effective magnetic moment calculated for the LiNc-BuO (T_g) was 1.56 μB per formula unit, which was smaller than the expected value of 1.73 μB for a spin system with $S = 1/2$. The crystals showed a single, sharp EPR spectrum with an unusually low line width of 20 ± 5 mG under anoxic conditions. The EPR line width was linearly dependent on partial pressure of oxygen (pO_2) in the range 0−760 mmHg, with a sensitivity of 4.54 ± 0.50 mG/mmHg. The LiNc-BuO (T_g) crystals possess several desirable properties for use as a probe for EPR oximetry.

Introduction

Metal complexes of phthalo- and naphthalocyanines have drawn substantial attention for their unique optical, magnetic, and electrical properties.[1−3] Interestingly, the myriad of properties of these complexes are attributed to their ability to exhibit polymorphism in the crystalline packing.[4] Polymorphism is due to different packing arrangements of a molecule in the solid state resulting in different intermolecular interactions and, therefore, different electronic and vibronic properties for each crystalline form. When considering metallo-phthalocyanines for applications as functional materials, it is particularly important to take into account the molecular structure, metal ions, and substituents, as well as the properties of the crystal structure such as interplanar spacing, molecular orientations, intermolecular interactions, and mobility of the charge carriers.[4] Thus, a thorough understanding of the properties of these polymorphic materials requires the knowledge of their molecular and crystal structures.

Of particular interest is the effect of polymorphism on the magnetic properties of paramagnetic phthalo- and naphthalocyanines. For example, paramagnetic copper-(II) phthalocyanines are known to have as many as ten polymorphic forms with distinct magnetic properties.[4] Structural polymorphism has also been reported in the case of paramagnetic LiPc, a monovalent lithium (Li^+) complex of phthalocyanine radical ($Pc^{\cdot-}$).[5] LiPc is an extremely stable solid that exhibits three distinct crystalline polymorphisms, namely α, β, and x forms, all of which are paramagnetic and EPR (electron paramagnetic resonance) active.[6] LiPc is one of the first stable neutral radicals that exhibits an intrinsic semiconducting behavior with unusual magnetic properties.[7] The x form of LiPc has been characterized to exhibit a single narrow EPR absorption with molecular oxygen concentration-dependent changes in line width, an interesting observation

*Corresponding author. Address: 420 West 12th Avenue, Room 114, Ohio State University, Columbus, OH 43210, USA. Fax: 614-292-8454; Tel: 614-292-8998; E-mail: kuppusamy.1@osu.edu.

(1) Armstrong, N. R. *J. Porphyrins Phthalocyanines* **2000**, *4*, 414–417.
(2) McKeown, N. B. *Phthalocyanine Materials: Synthesis, Structure and Function*; University Press: Cambridge, 1998.
(3) Moser, F. H.; Thomas, A. L. *The Phthalocyanine*; CRC Press: Boca Raton, FL, 1983; Vol. *1*−*2*.
(4) Kadish, K. M.; Smith, K. M.; Guilard, R. *The Porphyrin Handbook*; Academic Press: San Diego, CA, 2003; Vol. *20*, pp 1−242.
(5) Sugimoto, H.; Mori, M.; Masuda, H.; Taga, T. *J. Chem. Soc. Chem Commun.* **1986**, 962–963.
(6) Brinkmann, M.; Turek, P.; Andre, J. J. *J. Mater. Chem.* **1998**, *8*, 675–685.
(7) Turek, P.; Andre, J. J.; Giraudeau, A.; Simon, J. *Chem. Phys. Lett.* **1987**, *134*, 471–475.

Published on Web 11/02/2010

that led to its use as an oxygen-sensing probe for measurements of oxygen concentration (EPR oximetry) in tissues.[8]

Our laboratory has been interested in the development of paramagnetic crystals of monolithium phthalo- and naphthalocyanines for use as oxygen sensors in EPR oximetry.[9] A unique characteristic of these paramagnetic materials is that they exist in columnar crystalline packing and exhibit a single EPR absorption peak with unusually narrow line shape, attributed to Heisenberg spin-exchange interaction between the spins along the stack.[10] In addition, the columnar packing leads to the formation of open channels large enough for small paramagnetic gaseous molecules such as molecular oxygen (O_2) and nitric oxide (NO) to diffuse into the crystal and induce perturbation to the intrinsic spin-exchange, which is measurable as a T_2*-broadening in the observed EPR spectrum.[9] The EPR line-broadening effect of oxygen is quantitative and proportional to the partial pressure of molecular oxygen (pO_2) in the immediate environment of the crystal. The crystals are, thus, useful for the determination of oxygen concentration, a procedure referred to as EPR oximetry.[9,11] In the past, we have reported the synthesis, characterization, and oximetry evaluation of lithium phthalocyanine (LiPc),[12−14] lithium α-phenoxy-phthalocyanine (LiPc-α-OPh),[15] lithium naphthalocyanine (LiNc),[16−18] and lithium octa-*n*-butoxy-naphthalocyanine (LiNc-BuO)[19−21] crystals. Of these materials, we observed LiNc-BuO to have the most desirable properties for biological oximetry applications. LiNc-BuO is obtained as needle-shaped crystals. X-ray powder diffraction analysis indicated a triclinic (T_c) unit cell motif containing wide-open channels enabling a reversible transport (diffusion) of O_2 and NO molecules into the crystal.[19] We have used LiNc-BuO for a wide variety of biological oximetry applications including in vivo measurements.[22−31] Here we report the synthesis, structural, magnetic, and EPR characterization of a polymorph of LiNc-BuO. The polymorph is shown to have a tetragonal (T_g) unit packing with unusually sharp EPR absorption and with an EPR/oxygen sensitivity comparable to its T_c polymorph.

Materials and Methods

Tetrahydrofuran (THF), *n*-butanol, *n*-hexane, *n*-heptane, dichloromethane, silica gel, lithium granules, and 5,9,14,18,23,27,32,36-octa-*n*-butoxy-2,3-naphthalocyanine (Nc-BuO) were purchased from Sigma-Aldrich (St. Louis, MO).

Synthesis of Lithium 5,9,14,18,23,27,32,36-octa-*n*-butoxy-2,3-naphthalocyanine (LiNc-BuO) Radical. Lithium granules (0.0269 g, 3.871 mmol) were added to *n*-butanol (60 mL) and refluxed for 30 min under nitrogen atmosphere. The mixture was cooled to room temperature and Nc-BuO (0.5 g, 0.3871 mmol) was added and heated to 90 °C for 3 h under nitrogen atmosphere. After cooling to room temperature, 100 mL of *n*-heptane was added and the reaction mixture was passed through a silica-gel plug. The bright green solution was slowly evaporated under reduced pressure to obtain dark-green crystals of lithium 5,9,14,18,23,27,32,36-octa-*n*-butoxy-2,3-naphthalocyanine (LiNc-BuO). The crystals were washed with methanol and dried under vacuum. The yield was 86%. IR (KBr): ν = (3500−450 cm^{-1}), 2957, 2870, 1588, 1437, 1341, 1325, 1257, 1216, 1156, 1076, 996, 940, and 763 cm^{-1}. Elemental analysis of the product was in good agreement with the formula $C_{80}H_{88}N_8O_8Li$ (Calculated: C, 74.11; H, 6.84; N, 8.64; O, 9.87; Li, 0.54%. Found: C, 74.35; H, 6.93; N, 8.58; O, 9.42; Li, 0.55%). MS accurate−TOF-MS-ES^+: exact mass (m/z) calculated for $C_{80}H_{88}N_8O_8Li$ (M^+) 1296.6963; observed mass 1296.7135. The X-ray crystal structure analysis (*vide infra*) indicated that this material is a polymorph of LiNc-BuO that we have reported previously.[20]

(8) Liu, K. J.; Gast, P.; Moussavi, M.; Norby, S. W.; Vahidi, N.; Walczak, T.; Wu, M.; Swartz, H. M. *Proc. Natl. Acad. Sci. U.S.A.* **1993**, *90*, 5438–42.
(9) Ahmad, R.; Kuppusamy, P. *Chem. Rev.* **2010**, *110*, 3212–36.
(10) Turek, P.; Andre, J. J.; Simon, J. *Solid State Commun.* **1987**, *63*, 741–4.
(11) Swartz, H. M.; Boyer, S.; Gast, P.; Glockner, J. F.; Hu, H.; Liu, K. J.; Moussavi, M.; Norby, S. W.; Vahidi, N.; Walczak, T.; et al. ; et al. *Magn. Reson. Med.* **1991**, *20*, 333–9.
(12) Ilangovan, G.; Li, H.; Zweier, J. L.; Kuppusamy, P. *J. Phys. Chem. B* **2001**, *105*, 5323–5330.
(13) Ilangovan, G.; Zweier, J. L.; Kuppusamy, P. *J. Phys. Chem. B* **2000**, *104*, 9404–9410.
(14) Ilangovan, G.; Zweier, J. L.; Kuppusamy, P. *J. Phys. Chem. B* **2000**, *104*, 4047–4059.
(15) Pandian, R. P.; Dolgos, M.; Dang, V.; Sostaric, J. Z.; Woodward, P. M.; Kuppusamy, P. *Chem. Mater.* **2007**, *19*, 3545–3552.
(16) Ilangovan, G.; Manivannan, A.; Li, H.; Yanagi, H.; Zweier, J. L.; Kuppusamy, P. *Free Radical Biol. Med.* **2002**, *32*, 139–47.
(17) Manivannan, A.; Yanagi, H.; Ilangovan, G.; Kuppusamy, P. *J. Magn. Magn. Mater.* **2001**, *233*, L131–L135.
(18) Pandian, R. P.; Dolgos, M.; Marginean, C.; Woodward, P. M.; Chris Hammel, P.; Manoharan, P. T.; Kuppusamy, P. *J. Mater. Chem.* **2009**, *19*, 4138–4147.
(19) Pandian, R. P.; Kim, Y.; Woodward, P. M.; Zweier, J. L.; Manoharan, P. T.; Kuppusamy, P. *J. Mater. Chem.* **2006**, *16*, 3609–3618.
(20) Pandian, R. P.; Parinandi, N. L.; Ilangovan, G.; Zweier, J. L.; Kuppusamy, P. *Free Radical Biol. Med.* **2003**, *35*, 1138–48.
(21) Pandian, R. P.; Dang, V.; Manoharan, P. T.; Zweier, J. L.; Kuppusamy, P. *J. Magn. Reson.* **2006**, *181*, 154–61.
(22) Zhao, X.; He, G.; Chen, Y. R.; Pandian, R. P.; Kuppusamy, P.; Zweier, J. L. *Circulation* **2005**, *111*, 2966–72.
(23) Bratasz, A.; Pandian, R. P.; Deng, Y.; Petryakov, S.; Grecula, J. C.; Gupta, N.; Kuppusamy, P. *Magn. Reson. Med.* **2007**, *57*, 950–9.
(24) Chacko, S. M.; Khan, M.; Kuppusamy, M. L.; Pandian, R. P.; Varadharaj, S.; Selvendiran, K.; Bratasz, A.; Rivera, B. K.; Kuppusamy, P. *Am. J .Physiol. Heart Circ. Physiol.* **2009**, *296*, H1263–73.
(25) Khan, M.; Kutala, V. K.; Vikram, D. S.; Wisel, S.; Chacko, S. M.; Kuppusamy, M. L.; Mohan, I. K.; Zweier, J. L.; Kwiatkowski, P.; Kuppusamy, P. *Am. J. Physiol. Heart Circ. Physiol.* **2007**, *293*, H2129–39.
(26) Pandian, R. P.; Kutala, V. K.; Parinandi, N. L.; Zweier, J. L.; Kuppusamy, P. *Arch. Biochem. Biophys.* **2003**, *420*, 169–75.
(27) Takeshita, K.; Kawaguchi, K.; Fujii-Aikawa, K.; Ueno, M.; Okazaki, S.; Ono, M.; Krishna, M. C.; Kuppusamy, P.; Ozawa, T.; Ikota, N. *Cancer Res.* **2010**, *70*, 4133–40.
(28) Khan, M.; Meduru, S.; Mostafa, M.; Khan, S.; Hideg, K.; Kuppusamy, P. *J. Pharmacol. Exp. Ther.* **2010**, *333*, 421–9.
(29) Wisel, S.; Chacko, S. M.; Kuppusamy, M. L.; Pandian, R. P.; Khan, M.; Kutala, V. K.; Burry, R. W.; Sun, B.; Kwiatkowski, P.; Kuppusamy, P. *Am. J. Physiol. Heart Circ. Physiol.* **2007**, *292*, H1254–61.
(30) Khan, M.; Meduru, S.; Mohan, I. K.; Kuppusamy, M. L.; Wisel, S.; Kulkarni, A.; Rivera, B. K.; Hamlin, R. L.; Kuppusamy, P. *J. Mol. Cell Cardiol.* **2009**, *47*, 275–87.
(31) Mohan, I. K.; Khan, M.; Wisel, S.; Selvendiran, K.; Sridhar, A.; Carnes, C. A.; Bognar, B.; Kalai, T.; Hideg, K.; Kuppusamy, P. *Am. J. Physiol. Heart Circ. Physiol.* **2009**, *296*, H140–51.

Hence we used the abbreviation LiNc-BuO (T_g, tetragonal) for the new material and LiNc-BuO (T_c, triclinic) for the previously reported compound.

UV−visible−Near IR Measurements. The solid-state UV−visible−near IR absorption spectra of T_g and T_c polymorphs were obtained using a PerkinElmer Lambda 950 UV−visible−near IR spectrophotometer.

Single Crystal X-ray Diffraction Measurements and Analysis. The crystal used for X-ray single crystal data collection was a dark-green block. Because these crystals diffracted weakly, a synchrotron data set was collected. Intensity data were collected at 150 K on a D8 goniostat equipped with a Bruker APEXII CCD detector at Beamline 11.3.1 at the Advanced Light Source (Lawrence Berkeley National Laboratory) using synchrotron radiation tuned to $\lambda = 0.7749$ Å. For data collection, frames were measured with a frame width of 0.3° in ω and an exposure time of 1 s per frame for low-angle data and 5 s per frame for high-angle data out to a maximum 2θ value of 58°. The data frames were collected using the program APEX2 and integrated using the program SAINT within APEX2. The data were corrected for absorption and beam corrections based on the multiscan technique as implemented in SADABS.[32,33]

The structure was solved by the direct methods procedure in SHELXS-97[34] in space group $P4_12_12$. Full-matrix least-squares refinements based on F^2 were performed in SHELXL-97,[34] as incorporated in the WinGX package.[35] The molecule contains a crystallographic 2-fold rotation axis which passes through atoms Li, N(4) and N(5). One of the *n*-butyl groups is disordered over two sites with one orientation consisting of atoms C(37), C(38), C(39), and C(40), and the other orientation containing atoms C(37A), C(38A), C(39), and C(40A). The sum of the site occupancy factors for these two sites was constrained to be equal to 1.0. The occupancy factor for the first group [C(37), C(38), and C(40)] refined to 0.544(9), whereas that for the second group [C(37A), C(38A), and C(40A)] is 0.456(9). Since atom C(39) is common to both orientations, its occupancy factor was fixed at 1.0. Similar restraints were used in the refinement of these disordered chains, where the bond lengths for O4−C37 and O4−37A were restrained to be equal within a standard uncertainty of 0.01 Å (SADI restraints). Restraints for a specific value of a bond length or distance were used for the following: 1.50 Å for C39−C40A, 1.54 Å for C38−C39, C38A−C39, and C37−C38, and 2.60 for the distance between C38A and C40A (DFIX restraints, all with a standard uncertainty of 0.01 Å).

For each methyl group, the hydrogen atoms were added at calculated positions using a riding model with U(H) = 1.5* U_{eq} (bonded carbon atom). The remaining hydrogen atoms were included in the model at calculated positions using a riding model with U(H) = 1.2 * U_{eq}-(attached atom). The final refinement cycle was based on 7085 intensities, 8 restraints, and 462 variables, and resulted in agreement factors of R1(F) = 0.159 and wR2(F^2) = 0.250. For the subset of data with $I > 2$*sigma (I), the R1(F) value is 0.072 for 3180 reflections. The final difference electron density map contains maximum and minimum peak heights of 0.36 and −0.20 e/Å^3. Neutral atom scattering factors were used and include terms for anomalous dispersion.[36]

Magnetic Susceptibility Measurements. Magnetic susceptibility measurements were carried out on a polycrystalline powder sample of LiNc-BuO (T_g) at a field of 1000 G using a Quantum Design MPMS-5 superconducting quantum interference device (SQUID) magnetometer. Molar susceptibilities are given in emu G^{-1} mol^{-1}. Magnetic moments in Bohr Magnetons were calculated according to the relation $\mu = 2.84(\chi_m T)^{1/2}$. The powder LiNc-BuO ($T_g$) sample (~49 mg) was sealed in a quartz tube under vacuum (~10^{-3} Torr). The measured magnetic susceptibility values were corrected for diamagnetism, χ_D, using experimentally determined diamagnetic susceptibility of a metal-free reference compound Nc-BuO.

EPR Measurements. EPR measurements were performed using a Bruker ER300 spectrometer operating at X-band (9.78 GHz). Unless mentioned otherwise, the EPR linewidths reported are peak-to-peak width (ΔB_{pp}) of the first-derivative spectra. Spin density of LiNc-BuO (T_g) was determined by comparing the intensities of the EPR spectra of the LiNc-BuO (T_g) with DPPH measured under identical experimental conditions. EPR line width versus oxygen-partial-pressure (pO_2) calibration curves were constructed using X-band EPR measurements on the LiNc-BuO (T_g) crystals equilibrated with oxygen/nitrogen gas mixture as reported previously.[20]

Results and Discussion

Synthesis and Characterization of LiNc-BuO (T_g) Polymorph. LiNc-BuO (T_g) was synthesized by reacting Nc-BuO with metallic lithium in *n*-butanol. The compound was obtained by recrystallization from *n*-heptane/*n*-butanol mixture as dark-green, diamond-shaped microcrystals (Figure 1A). The shape of LiNc-BuO (T_g) form was different from that of LiNc-BuO (T_c) which showed needle-shaped crystals. Elemental analysis, IR, and UV−visible spectroscopic data of LiNc-BuO (T_g) were in accordance with the proposed molecular structure. The absence of the 3297-cm^{-1} band corresponding to the NH stretching absorption in the IR spectrum (data not shown) indicated the absence of the metal-free form, Nc-BuO, in the product. LiNc-BuO (T_g) was quite stable in the solid-state form, from room temperature to 250 °C. The crystals were soluble in most of the common, nonpolar organic solvents, such as *n*-hexane, *n*-heptane, and

(32) *APEX2 v2008.6.0 and SAINT v7.46A data collection and data processing programs*; Bruker Analytical X-ray Instruments, Inc.: Madison, WI; (b) *SADABS v2008/1 semi-empirical absorption and beam correction program*; Sheldrick, G.M.; University of Göttingen: Germany.
(33) Sheldrick, G. M. *SADABS v2008/1 semi-empirical absorption and beam correction program*; University of Göttingen: Germany, 2008.
(34) Sheldrick, G. M. *Acta Crystallogr.* **2008**, *A64*, 112–122.
(35) Farrugia, L. J. *J. Appl. Crystallogr.* **1999**, *32*, 837–838.
(36) *International Tables for Crystallography*; Kluwer Academic Publishers: Dordrecht, 1992; Vol. C.

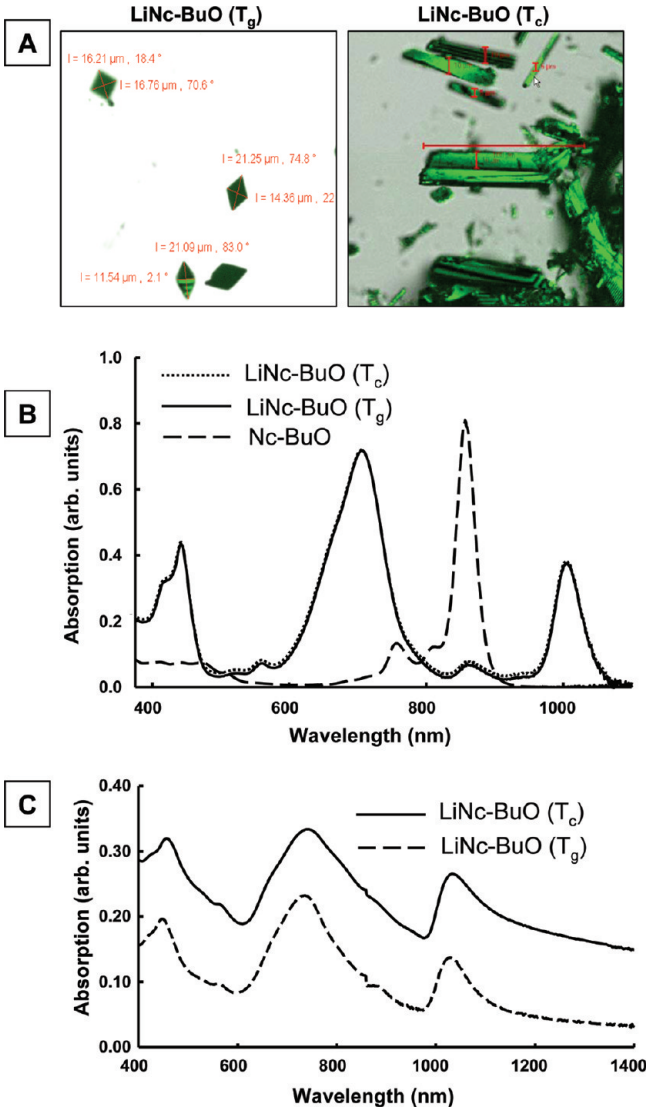

Figure 1. Microscopic images and optical spectra of LiNc-BuO (T_g) and LiNc-BuO (T_c). (A) Confocal images of crystalline polymorphs of LiNc-BuO. The T_g and T_c notation refers to tetragonal (this work) and triclinic[19,20] structural polymorphs of LiNc-BuO crystals. (B) UV−visible−near-infrared spectra of polymorphic forms of LiNc-BuO and metal-free Nc-BuO in THF solvent. The peak maxima are similar for both polymorphic T_g and T_c forms of LiNc-BuO suggesting that in the dissolved form the molecules are identical. The spectra show Q bands at 1005, 857 nm and 705 (broad) absorption bands that are bathochromic-shifted relative to the metal-free Nc-BuO. (C) Solid-state optical spectra of LiNc-BuO (T_g) and LiNc-BuO (T_c) at room temperature. The absorption maxima of T_g form of LiNc-BuO are 1029, 735 and 449, 423 (br.) nm. The absorption maxima for T_c form of LiNc-BuO are 1035, 745, 456, 427 (br.) nm. The spectra show a blue-shift in the absorption maxima of LiNc (T_g) relative to LiNc-BuO (T_c).

dichloromethane. The solubility of LiNc-BuO (T_g) in organic solvents can be attributed to a reduction of the intermolecular interactions between naphthalocyanine rings, possibly due to the butoxy groups (*vide infra*). The solubility of LiNc-BuO (T_g) in organic solvents is similar to that of LiNc-BuO (T_c),[20] but in contrast to LiNc[18] and LiPc,[14,37] which were insoluble. The solubility of LiNc-BuO (T_g) in organic solvents enabled easy purification of it using column chromatography and subsequent recrystallization.

Optical Properties of LiNc-BuO in Solution. The UV−visible absorption spectrum of the T_g form of LiNc-BuO in THF was obtained using a Varian Cary 50 UV−visible spectrophotometer. Figure 1B shows the spectrum of LiNc-BuO (T_g) as well as LiNc-BuO (T_c) and Nc-BuO for comparison. The T_g form showed Q bands at 1005, 857, and 705 (broad) nm and a weak split Soret band at 449 nm. The Nc-BuO showed a strong Q-band at 865 nm.[38,39] The absorption bands of the T_g form of LiNc-BuO are bathochromically shifted relative to the unsubstituted lithium naphthalocyanine (LiNc)[16,17,40] and Nc-BuO. It should be further noted that both the T_g and T_c forms of LiNc-BuO have similar absorption bands in solution suggesting that they are identical in the molecular form.

Optical Properties of Polymorphs of LiNc-BuO in Solid State. The solid-state optical spectra of LiNc-BuO (T_g) and LiNc-BuO (T_c) are shown in Figure 1C. The solid-state optical spectra showed important differences in the near IR region, Q and X bands of the absorption spectra between the T_g and the T_c forms of LiNc-BuO. The absorption maxima of the T_g form were 1029, 735 and 449, 423 (br.) nm. The absorption maxima of the T_c form were 1035, 745, 456, 427 (br.) nm. The absorption maxima of the T_g polymorph was blue-shifted relative to the T_c polymorph. Those differences are explained qualitatively by means of symmetry as well as energy level changes in $\pi-\pi$ stacking of molecules in the crystalline packing environment. The blue shift observed in the absorption maxima of T_g relative to T_c polymorph indicates that HOMO − LUMO gap is increased in the T_g in comparison to T_c polymorph. The observed changes in optical spectra of T_g and T_c polymorphs of LiNc-BuO are similar to those observed in α, β, and x forms of LiPc.[41−43]

Crystal and Molecular Structure. Table 1 contains the crystallographic details of LiNc-BuO (T_g). The molecule crystallizes in the tetragonal space group $P4_12_12$ and it contains a crystallographic, 2-fold rotation axis which passes through atoms Li, N(4), and N(5). As a result of this symmetry, the central core of the molecule containing the Li, N(1), N(3), N(1′), and N(3′) atoms is approximately planar. Two views of the molecule are shown in Figure 2 (A and B). In Figure 2B, the side-on view indicates a slightly distorted saddle conformation for the naphthalocyanine moiety. Each "benzo-isoindole" ring is oriented up and down in an alternate manner with respect to the plane of the central core (Li, N(1), N(3),

(37) Afeworki, M.; Miller, N. R.; Devasahayam, N.; Cook, J.; Mitchell, J. B.; Subramanian, S.; Krishna, M. C. *Free Radical Biol. Med.* **1998**, *25*, 72–78.
(38) Cook, M. J.; Dunn, A. J.; Howe, S. D.; Thomson, A. J.; Harrison, K. J. *J. Chem. Soc., Perkin Trans. 1* **1988**, 2453–2458.
(39) Rihter, B. D.; Kenney, M. E.; Ford, W. E.; Rodgers, M. A. J. *J. Am. Chem. Soc.* **1993**, *115*, 8146–8152.
(40) Manivannan, A.; Yanagi, H. *Chem. Lett.* **2001**, 568–569.
(41) Brinkmann, M.; Choumant, C.; Wachtel, H.; Andre, J. J. *Thin Solid Films* **1996**, *283*, 97.
(42) Sumimoto, M.; Sakaki, S.; Matsuzaki, S.; Fujimoto, H. *J. Chem. Soc., Dalton Trans.* **2003**, 31.
(43) Wachtel, H.; Wittmann, J. C.; Lotz, B.; Petit, M.; Andre, J. J. *Thin Solid Films* **1994**, *250*, 219.

Table 1. Crystallographic Details for T_g Form of LiNc-BuO

formula	$C_{80}H_{88}LiN_8O_8$
formula weight	1296.569
temperature	150(2) K
wavelength	0.77490 Å
crystal system	tetragonal
space group	$P4_12_12$
unit cell dimensions	a = 15.436(1) Å; c = 28.831(2) Å
volume	6869.6(8) Å^3
Z	4
density (calculated)	1.254 Mg/m^3
absorption coefficient	0.066 mm^{-1}
F(000)	2764
crystal size	0.05 × 0.07 × 0.11 mm^3
theta range for data collection	2.55 to 29.04°
index ranges	$-19 \le h \le 19$, $-19 \le k \le 19$, $-36 \le l \le 36$
reflections collected	104308
independent reflections	7085 [R(int) = 0.125]
completeness to theta = 29.04°	99.9%
refinement method	full-matrix least-squares on F^2
data/restraints/parameters	7085/8/462
goodness-of-fit on F^2	0.996
final R indices [I > 2sigma(I)]	$R1$ = 0.0720, w$R2$ = 0.1896
R indices (all data)	$R1$ = 0.1586, w$R2$ = 0.2496
largest diff. peak and hole	0.356 and −0.196 e/Å^3

N(1′), and N(3′)). The dihedral angle between the "benzoisoindole" ring and the plane of the central core is 5.2° for the ring containing N(1) and 8.3° for the ring containing N(3). Intramolecular steric interactions are such that if one butoxy group extends above the core of the molecule, the neighboring butoxy group extends below the core of the molecule.

Among the neutral naphthalocyanine radicals, this represents the first single crystal structure of a substituted lithium naphthalocyanine complex. The packing of the molecules within the unit cell is complex and is best understood by describing the layers formed by the lithium atoms, which are perpendicular to the c axis. These layers are color-coded in the packing plot in Figure 2C. The molecules that contain Li atoms at z = 0 and z = 1 are colored red, those at z = 1/4 are blue, at z = 1/2 are yellow, and at z = 3/4 are green. The molecules are tilted with respect to the ab plane and this tilt is described by the angle between the plane of the central core through the Li, N(1), N(3), N(1′), and N(3′) atoms and the ab plane. This angle is always 21.2°. Within any one layer there is a set of parallel planes consisting of the planes through various central core sets of Li, N(1), N(3), N(1′), and N(3′) atoms. In Figure 2C, two of these planes are shown edge-on for the z = 0 layer, and the distance between these two planes is 3.954 Å. Every layer (at z = 1/4, z = 1/2, and z = 3/4) has this feature of parallel planes at 3.954 Å apart. The dihedral angle between two least-squares planes of adjacent layers (for example, the layers at z = 0 and z = 1/4) is 29.7°.

A space-filling representation of the crystal structure looking down the b-axis is shown in Figure 3. The atomic packing is fairly efficient with very small channels that extend parallel to the a and b axes. It is not obvious to what extent small molecules, such as O_2, can diffuse through these channels. A view of the structure parallel to the c axis does not show any channels for diffusion of small molecules. Like other lithium phthalocyanines, for

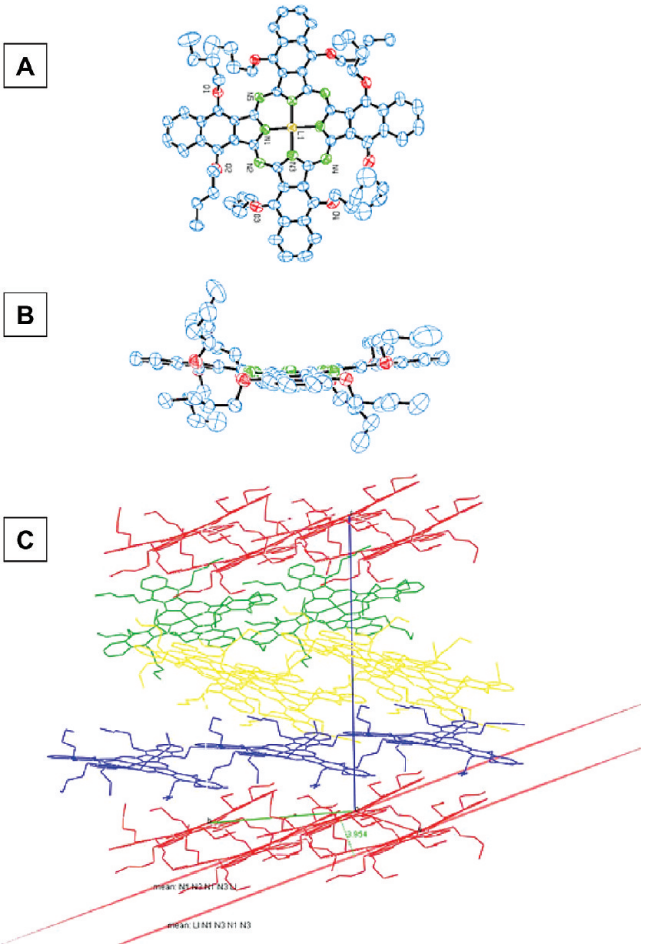

Figure 2. Molecular structure and crystalline packing of LiNc-BuO (T_g). (A) Top view of the molecular structure. The ORTEP plot is drawn with 30% probability ellipsoids for the non-hydrogen atoms. The hydrogen atoms are omitted for clarity. Only one of the disordered butyl groups bonded to the O(4) atom is shown. The molecule contains a crystallographic 2-fold rotation axis, which contains the Li, N(4), and N(5) atoms. (B) Side view of the molecular structure of LiNc-BuO with 30% probability ellipsoids. This view of the molecule shows the saddle conformation. The hydrogen atoms are omitted for clarity. (C) Crystalline packing of LiNc-BuO. Slip-stacked pattern along the crystallographic ab plane. The unit-cell-packing plot is color-coded with respect to the Li atom positions. The red molecules contain Li atoms at z = 0 and z = 1, blue molecules have Li atoms at z = 1/4, yellow molecules at z = 1/2, and green molecules at z = 3/4. Hydrogen atoms are omitted for clarity.

example LiPc,[6] LiNc-BuO is polymorphic. The crystalline packing of LiNc-BuO (T_c) was previously reported to be triclinic.[19] A comparison of the T_g- and T_c-polymorphs is shown in Figure 4. Due to the lack of suitable single crystals, the conformation of the butoxy groups of the T_c form is not accurately known. Nonetheless, a comparison of the packing of the conjugated lithium naphthalocyanine moieties (LiNc) of the two structures is instructive (Table 2). The molecules in the triclinic polymorph lie parallel to each other in slip-stacked columns. This pattern of molecular packing is likely favored by strong intermolecular $\pi-\pi$ stacking interactions. In contrast, planes of neighboring molecules in the T_g-polymorph are tilted with respect to one another as described above. Whereas molecules in the T_c polymorph form a sort of dimer with Li−Li contacts of 5.4 Å, the shortest Li−Li contacts in the T_g-polymorph are 11.2 Å.

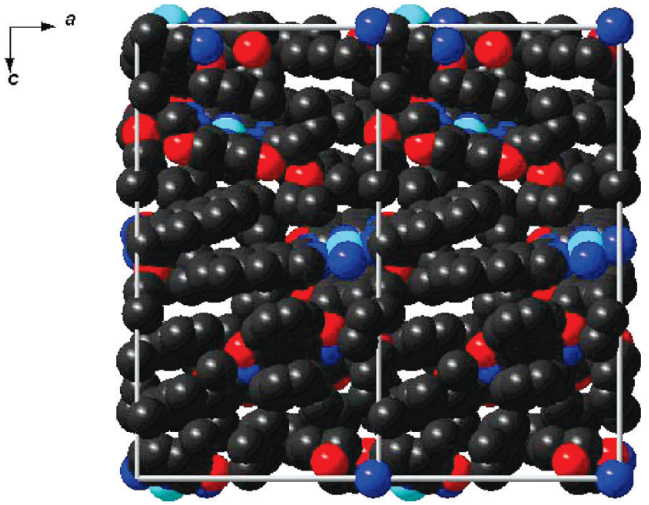

Figure 3. Three-dimensional representation of the atomic packing in LiNc-BuO (T_g). A space-filling view of the atoms in a four-unit-cell block demonstrates the relatively efficient packing.

The butoxy groups that extend off of the planar portion of the molecule interfere with the stacking normally seen in phthalocyanines and naphthalocyanines. While $\pi-\pi$ slip stacking is still operative in the T_c form of LiNc-BuO, this does not lead to optimal packing of the butoxy portion of the molecule. In the T_g form of LiNc-BuO the molecules find a way to pack more densely, but it seems to disrupt the nice $\pi-\pi$ stacking patterns normally seen with molecules of this type. Figure B in the Supporting Information shows only the Li ions and the immediately surrounding N and C rings and shows that the usual $\pi-\pi$ stacking is absent in the T_g form of LiNc-BuO. Figure 2 shows the limited $\pi-\pi$ interactions between molecules in the same layer (in the *xy* plane) and involving stacking between the outer conjugated regions of each molecule. The slipping distance in the T_g form of LiNc-BuO is relatively larger, and can be attributed to substantial steric interaction by the butoxy groups, which is absent in the case of LiPc.

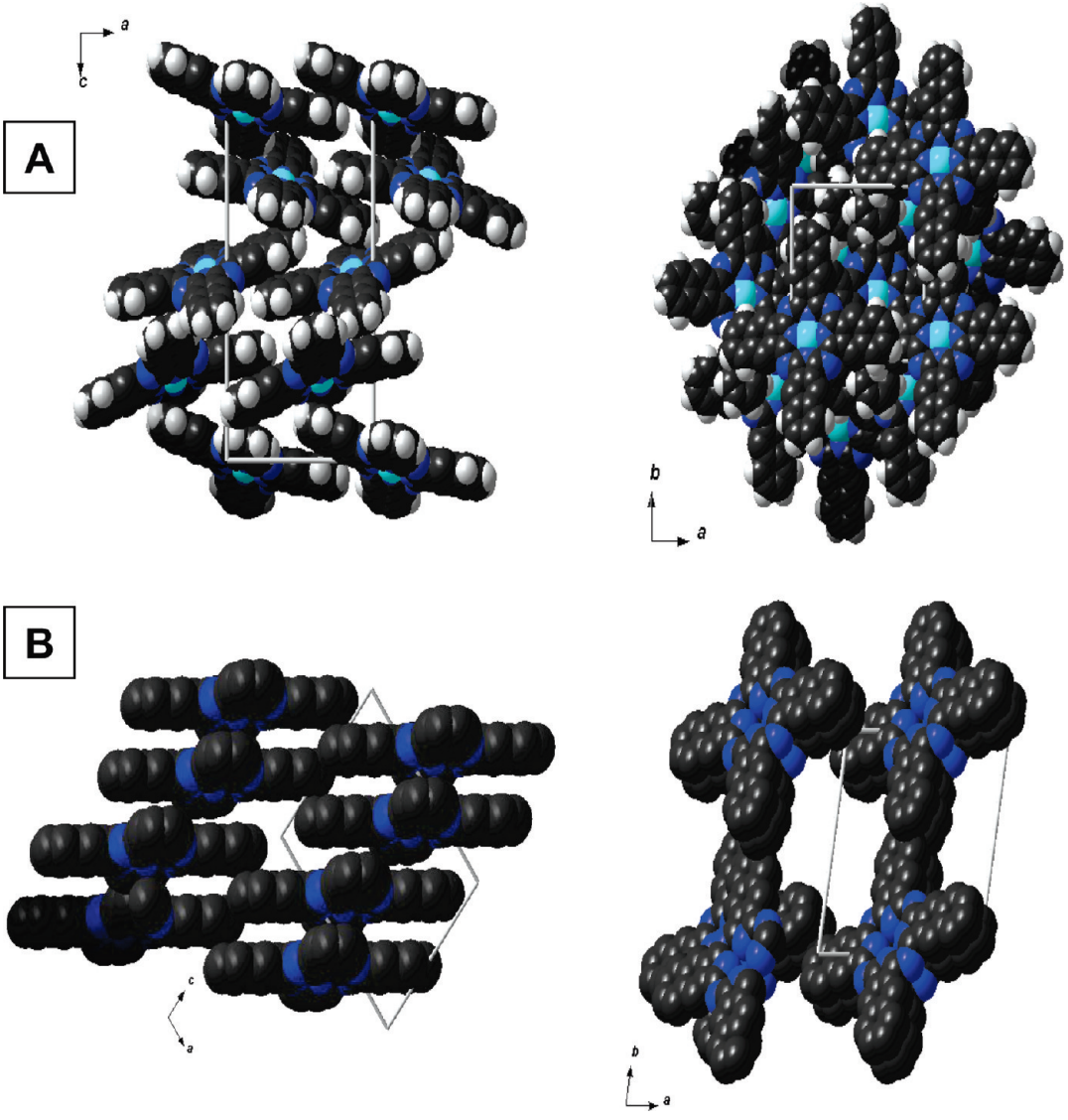

Figure 4. Molecular packing of LiNc-BuO in the T_g and T_c crystalline polymorphs. (A) LiNc-BuO (T_g). (B) LiNc-BuO (T_c). In the molecular packing shown in (A), the butoxy groups are not shown for clarity and for the sake of comparison with the T_c-polymorph where the positions of the butoxy groups are not known.

Table 2. Comparison of Properties of LiPc, LiPc-α-OPh, LiNc, and Polymorphs of LiNc-BuO Lattices

parameter	LiPc	LiPc-α-OPh	LiNc	LiNc-BuO (T_c)	LiNc-BuO (T_g)
slipping distance (Å)	-	4.65	1.56	4.7	
interstack or interplanar distance (Å)	3.25	3.36	3.45	4.7	3.95
channel size (cross-sectional diameters, Å)	6 × 6	4.9 × 4.6 4.6 × 8.7	5.0 × 5.4	10 × 6 6 × 4 5 × 5	-

The lack of accurate positions for the butoxy chains in the T_c form of LiNc-BuO makes it difficult to directly compare the channels/porosity of the two polymorphs. However, when the butoxy groups are omitted, as they are in Figure 3, the T_c-polymorph appears to have much more favorable channels for small-molecule diffusion. A comparison of the molar volume of the two polymorphs is also instructive. The triclinic T_c-polymorph has volume of 1935 Å^3 per molecule, whereas the tetragonal T_g-polymorph has a volume of 1717 Å^3 per molecule. The observation that the T_g-polymorph is 11% more dense suggests that the T_c-polymorph is more porous. Although the saddle conformation adopted by LiNc-BuO (T_g) is not conducive to π stacking, some $\pi-\pi$ interactions probably exist between naphthalocyanine molecules because of the 3.332 Å distance between two overlapped benzo-isoindole sections of neighboring molecules (Figure 2C).

Magnetic Susceptibility. The magnetic susceptibility studies of phthalocyanine and their benzoannulated derivatives have been extensively documented in the literature.[44,45] The magnetism of these conjugated metal complexes has been studied either on highly doped or poorly characterized metallo-phthalocyanines.[44,45] However, the magnetic susceptibility studies of thoroughly characterized neutral radicals of lithium metal derivatives of phthalocyanine and naphthalocyanine are very limited.[18,46,47] By studying the temperature-dependent bulk susceptibility, as well as the crystal structure, it is possible to obtain important insight regarding the magnetic coupling between neighbors or within a column of molecules. Furthermore, the spin dynamics of the system have to be correctly inferred. This will throw substantial light on the nature of magnetism in the condensed phase as well as reveal the nature of spin dynamics.

We have studied the magnetic susceptibility of LiNc-BuO (T_g) under anoxic conditions from ambient temperature to 5 K using a SQUID magnetometer. The susceptibility data were corrected for the diamagnetic background using the experimentally determined diamagnetic susceptibility of a metal-free reference compound Nc-BuO. Inverse molar susceptibility plotted as a function of temperature (Figure 5A) followed the Curie−Weiss law $\chi = C/(T - \theta)$ in the temperature range from 300 K to about 50 K. The Curie constant, $C = 0.303(1)$ emu·K/mol,

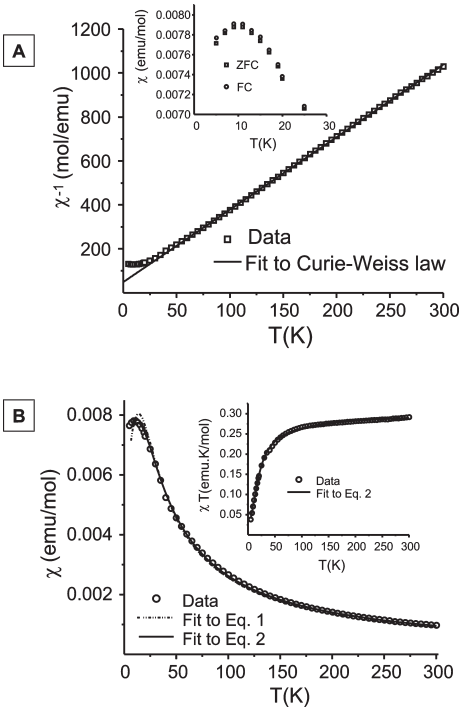

Figure 5. Magnetic susceptibility of LiNc-BuO (T_g). (A) Variation of inverse molar susceptibility with temperature under an applied magnetic field of 1000 G. The experimental (□) and theoretical (−) values fit to the Curie−Weiss law are given for comparison. The experimental susceptibility values have been corrected for diamagnetism. ZFC and FC susceptibility data are shown in the inset. (B) Variation of molar susceptibility with temperature under an applied magnetic field of 1000 G. The experimental (○) and theoretical (−) values fit to the Curie law are given for comparison. See text for the explanation of eqs 1 and 2. Inset shows χT product as a function of temperature. The experimental susceptibility values have been corrected for diamagnetism.

obtained from the fitting procedure corresponded to an effective magnetic moment of 1.56 μB per formula unit which is smaller than an expected value of 1.73 μB for a spin system with $S = 1/2$ and a g value of 2.0027. The Weiss constant, $\theta = -14.7(1)$ K, indicated antiferromagnetic interactions. ZFC and FC susceptibility variations with temperature followed a similar behavior as shown in the inset of Figure 5A. The susceptibility variation with temperature (Figure 5B) registered a broad maximum at ~10 K indicating an antiferromagnetic-like ordering. Despite the slight saddle deformation of the molecule in the solid state, LiNc-BuO (T_g) does show $\pi-\pi$ stacking interactions. The spin exchange is consistent with the existence of well-separated stacks and that favor a high degree of spin exchange. The effective $\pi-\pi$ interactions exist between the neighboring naphthalocyanine molecules due to the short distance between them with a separation of 3.332 Å. We fit the data to the Heisenberg one-dimensional

(44) Inabe, T. *J. Porphyins Phthalocyanines* **2001**, *5*, 3–12.
(45) Inabe, T.; Tajima, H. *Chem. Rev.* **2004**, *104*, 5503–34.
(46) Brinkmann, M.; Andre, J. J. *J. Mater. Chem.* **1999**, *9*, 1511–1520.
(47) Dumm, M.; Dressel, M.; Nicklas, M.; Lunkenheimer, P.; Loidl, A.; Weiden, M.; Steglich, F.; Assmann, B.; Homborg, H.; Fulde, P. *Eur. Phys. J. B: Condens. Matter Phys.* **1998**, *6*, 317–322.

antiferromagnetic chain model (the Bonner−Fisher model)[48] using the numerical expression

$$\chi = \frac{Ng^2\mu_B^2}{k_BT}\left(\frac{0.25+0.074975x+0.075235x^2}{1.0+0.9931x+0.172135x^2+0.757825x^3}\right)\cdots \quad (1)$$

where $x = |J|/T$ and J is antiferromagnetic exchange constant between the nearest neighbor spins in the linear chain.[49]

As can be seen from the Figure 5B, the fitting obtained from the above eq 1 traces the experimentally observed maximum closely. However, below the susceptibility maximum 10 K, the susceptibility data decrease rather slowly with temperature compared to the calculated values from the eq 1. This type of behavior at lower temperatures is often found in spin systems with a singlet ground state due to the presence of a small amount of noncoupled spins in the sample. To take the uncoupled spins into account a second Curie term is added to the eq 1 as follows:

$$\chi = \frac{Ng^2\mu_B^2}{k_BT}\left(\frac{0.25+0.074975x+0.075235x^2}{1.0+0.9931x+0.172135x^2+0.757825x^3}\right)(1-\rho) + \frac{Ng^2\mu_B^2}{k_BT}\rho\cdots \quad (2)$$

where ρ is the molar fraction of the noncoupled spins. This correction for the noncoupled spins significantly improves the fitting of the data validating the assumption of noncoupled spins in the sample. Molar fraction ρ determined from the fitting to eq 2 is only 0.008 but its contribution becomes increasingly significant as the temperature decreases. The fitting of the data to eq 2 gives an exchange constant $J = -21.3(3)$ K. The inset in Figure 5B displays the product χT, which is proportional to the effective magnetic moment, against temperature. From room temperature down to about 100 K, the effective magnetic moment reduced slowly from 1.53 to 1.46 μB per formula unit and below which it decreased rapidly with temperature due to the onset of antiparallel alignment of the spins within the linear chains.

EPR Properties. Table 3 shows a comparison of anoxic linewidths of some known lithium phthlocyanine-based EPR probes with the T_g polymorph of LiNc-BuO. The LiNc-BuO (T_g) microcrystals, under anoxic conditions, exhibited a single, sharp peak with a peak-to-peak width of 20 ± 5 mG (Figure 6A). The line width was comparable to that of LiPc.[8,14,37] LiPc also crystallizes in a tetragonal unit cell (x form) with straight molecular packing along the c axis and with an interplanar LiPc−LiPc spacing of 3.245 Å compared to 3.95 Å in the case of LiNc-BuO (T_g).[5] The straight columnar packing of LiPc leads to channels of approximately 6 Å diameter along the stack axis. The T_g form of LiNc-BuO presents a markedly different molecular packing pattern from that of LiPc. The subtle increase in stacking distance and/or the inductive effect caused by the increase in the butoxy groups, as well as in mobile π electrons due to benzoannulation in the T_g form of LiNc-BuO could be responsible for the shorter EPR line width. The steric butoxy groups in the T_g form of LiNc-BuO may release a substantial amount of the electron density to the naphthalocyanine moiety, leading to significant acceleration of spin diffusion along the a-axis. Moreover, the triclinic T_c-polymorph has a volume of 1935 Å^3 per molecule, while the tetragonal T_g-polymorph has a volume of 1717 Å^3 per molecule (as noted earlier the T_g-polymorph is 11% more dense than the T_c-polymorph). These effects may account for the low anoxic line width (20 ± 5 mG) in comparison to the T_c form of LiNc-BuO,[20] LiNc[18], and LiPc-α-OPh.[15] The spin density, calculated from the intensity ratio with the standard diphenylpicrylhydrazyl (DPPH) radical, was $7.5 \pm 0.2 \times 10^{20}$ spins/g. This value is comparable to that reported for the T_c form of LiNc-BuO (7.2×10^{20} spins/g). The g value for the T_g polymorph of LiNc-BuO was found to be 2.0027 ± 0.0003, which is close to the free-electron value 2.0023.

Table 3. Comparison of Anoxic Line Width and Oxygen Sensitivity of Some Lithium Phthlocyanine and Lithium Naphthalocyanine Derivatives

spin probe	anoxic line width (mG)	oxygen sensitivity (mG/mmHg)	ref
LiPc	14 ± 2	6.1	Liu et al.[8]
LiPc	10−70	9.0−9.5	Ilangovan et al.[13]
LiPc	50	9.2	Afeworki et al.[37]
LiNc	630	31.2	Pandian et al.[18]
LiPc-α-OPh	530	13.7	Pandian et al.[15]
LiNc-BuO (T_c)	210	8.5	Pandian et al.[19]
LiNc-BuO (T_g)	20 ± 5	4.54 ± 0.50	present work

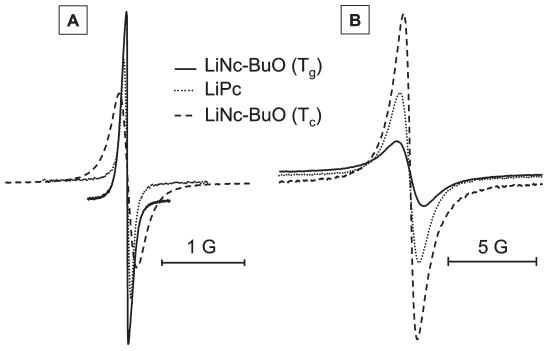

Figure 6. EPR spectra of T_c and T_g forms of LiNc-BuO and x form of LiPc crystals. The spectra were acquired using an X-band (9.78 GHz) EPR spectrometer at room temperature. (A) EPR spectra of the microcrystals under 100% nitrogen gas environment. The instrumental settings were as follows: microwave power, 0.1 mW; modulation amplitude 10 mG for LiNc-BuO (T_g) and LiPc (x), and 0.056 G for LiNc-BuO (T_c); modulation frequency, 100 kHz; receiver time constant, 41 ms; receiver gain, variable; acquisition time, 10 s (single scan). A single sharp peak is observed with a peak-to-peak width (ΔB_{pp}) of 20, 70, and 210 mG for LiNc-BuO (T_g), LiPc (x), and LiNc-BuO (T_c), respectively. (B) EPR spectra of the T_c and T_g polymorphic forms of LiNc-BuO and x form of LiPc crystal under room air (159 mmHg) environments. The instrumental settings were as follows: microwave power, 1 mW; modulation 200 mG, modulation frequency, 100 kHz; receiver time constant, 41 ms; receiver gain, variable; acquisition time, 10 s (single scan). A single sharp peak is observed with a peak a peak width (ΔB_{pp}) of 0.76, 1.05, and 1.52 G for T_g form of LiNc-BuO, LiPc, and T_c form of LiNc-BuO, respectively.

(48) Bonner, J. C.; Fisher, M. E. *Phys. Rev.* **1964**, *135*, A640–58.
(49) Estes, W. E.; Gavel, D. P.; Hatfield, W. E.; Hodgson, D. *Inorg. Chem.* **1978**, *17*, 1415–21.

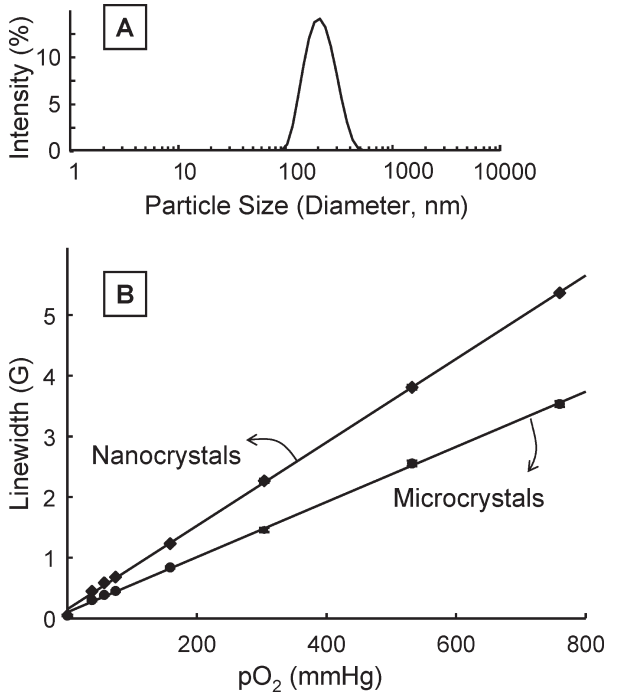

Figure 7. Crystal-size-dependent oxygen sensitivity of LiNc-BuO (T_g) crystals. (A) Size-distribution profile of LiNc-BuO (T_g) crystalline particles obtained by sonication of raw crystals. (B) Effect of molecular oxygen (pO_2) on the EPR line width of micro- (raw) and nano- (sonicated) crystals from a single batch. A linear variation of line width with the pO_2 is observed. The probe sensitivity (as measured by the slope) is 4.54 mG/mmHg for microcrystals and 6.87 mG/mmHg for sonicated nanocrystals.

Effect of Molecular Oxygen on the EPR Spectrum of LiNc-BuO (T_g). A comparison of EPR spectra of T_c and T_g polymorphs of LiNc-BuO and *x* form of LiPc crystal under anoxic and room air environments is shown in Figure 6. Table 3 shows a comparison of the oxygen sensitivities of lithium phthalocyanine-based probes with the T_g polymorph of LiNc-BuO. The EPR line width of LiNc-BuO (T_g) crystals exhibited a linear response to surrounding oxygen partial pressure (pO_2) (Figure 7). The linear variation in the entire 0−760 mmHg range would suggest that oxygen is transported freely into the crystals. The slope of 4.54 ± 0.50 mG/mmHg was comparable to that of LiPc (*x* form), but significantly less when compared to that of LiNc-BuO (T_c) (Table 3). A notable feature that is common to the phthalo- and naphthalocyanine paramagnetic crystals is the variation in crystal size, EPR line width, and oxygen sensitivity from batch to batch of preparation or recrystallization. LiNc-BuO (T_g) also exhibited small variations in crystal size and oxygen sensitivity among preparations, possibly due to disordered growth. We observed that reduction of crystal size, from several micrometers in the raw form to submicrometer levels by sonication, leads to reproducible line width and oxygen sensitivity. The particle-size distribution in LiNc-BuO (T_g) crystals, on sonication at 22.5 kHz, ranged from 100 to 500 nm, with a maximum number of particles at 205 nm. (Figure 7A). The sonicated particles retained both oxygen sensitivity and linearity in the line width-versus-pO_2 curve (Figure 7B). The slope of the line width−pO_2 curve, which reflects the oxygen sensitivity of the probe line width, was 6.87 mG/mmHg after sonication. The size reduction resulted in an increase of oxygen sensitivity. Despite the variability in the oxygen sensitivity among different batches, the crystals of T_g form of LiNc-BuO consistently exhibited an increase in oxygen sensitivity upon nanocrystal formation. A possible reason for this increase in oxygen sensitivity when decreasing the size of the crystals by sonication could be the increase in surface area of the crystals, and sonochemical effect of acoustic cavitations which could result in chemical reactions on the surface of the particles, resulting in opening of these channels in the crystal. The ability to form submicrometer-sized particles that remain sensitive to oxygen is particularly advantageous for intracellular internalization of these nanoparticles for cell-tracking or cellular oximetry applications.[23,50,29]

Summary and Conclusions

The synthesis, structural, and paramagnetic properties of a new tetragonal crystalline polymorph of lithium octa-*n*-butoxy-naphthalocyanine, LiNc-BuO (T_g), have been studied. The new material showed strikingly different oximetry properties from those of the previously known triclinic form, LiNc-BuO (T_c). Single-crystal X-ray diffraction analysis of LiNc-BuO (T_g) revealed a slightly distorted molecular structure with a saddle conformation. The spin exchange was in agreement with the X-ray crystal structure that showed the existence of well-separated stacks favoring a high degree of spin exchange in the lattice. The material possesses several desirable properties for use as a probe for EPR oximetry. The extremely narrow anoxic line shape combined with a low oxygen sensitivity may be particularly advantageous for applications that require the measurement of a wide range of oxygen concentrations.

Acknowledgment. This work was supported by NIH grant EB004031. We thank Dr. Jeanette Krause (University of Cincinnati) for the data collection through the SCrALS program, Ms. Gayatri Natu for solid state optical spectra measurements, and Mr. Brian Rivera for critical reading of the manuscript.

Supporting Information Available: Additional experimental data (pdf and cif). This material is available free of charge via the Internet at http://pubs.acs.org.

(50) Bratasz, A.; Pandian, R. P.; Ilangovan, G.; Kuppusamy, P. *Adv. Exp. Med. Biol.* **2006**, *578*, 375–80.